

Open

Original Article

The Chk1 inhibitor MK-8776 increases the radiosensitivity of human triple-negative breast cancer by inhibiting autophagy

Zhi-rui ZHOU^{1,2,#}, Zhao-zhi YANG^{1,2,#}, Shao-jia WANG^{2,3}, Li ZHANG^{1,2}, Ju-rui LUO^{1,2}, Yan FENG^{1,2}, Xiao-li YU^{1,2}, Xing-xing CHEN^{1,2,*}, Xiao-mao GUO^{1,2,*}

¹Department of Radiation Oncology, Fudan University Shanghai Cancer Center, Shanghai 200032, China; ²Department of Oncology, Shanghai Medical College, Fudan University, Shanghai 200032, China; ³Cancer Institute and Department of Gynaecological Oncology, Fudan University Shanghai Cancer Center, Shanghai 200032, China

Abstract

MK-8776 is a recently described inhibitor that is highly selective for checkpoint kinase 1 (Chk1), which can weaken the DNA repair capacity in cancer cells to achieve chemo-sensitization. A number of studies show that MK-8776 enhances the cytotoxicity of hydroxyurea and gemcitabine without increasing normal tissue toxicities. Thus far, there is no evidence that MK-8776 can be used as a radiotherapy sensitization agent. In this study, we investigated the effects of MK-8776 on the radiosensitivity of 3 human triple-negative breast cancer (TNBC) cell lines MDA-MB-231, BT-549 and CAL-51. MK-8776 dose-dependently inhibited the proliferation of MDA-MB-231, BT-549 and CAL-51 cells with IC₅₀ values of 9.4, 17.6 and 2.1 μmol/L, respectively. Compared with irradiation-alone treatment, pretreatment with a low dose of MK-8776 (100–400 nmol/L) significantly increased irradiation-induced γH2A.X foci in the 3 TNBC cell lines, suggesting enhanced DNA damage by MK-8776, inhibited the cell proliferation and increased the radiosensitivity of the 3 TNBC cell lines. Similar results were obtained in MDA-MB-231 xenograft tumors in nude mice that received MK-8776 (15 or 40 mg/kg, ip) 26 d after irradiation. To explore the mechanisms underlying the radio-sensitization by MK-8776, we used TEM and found that irradiation significantly increased the numbers of autophagosomes in the 3 TNBC cell lines. Moreover, irradiation markedly elevated the levels of Atg5, and promoted the transformation of LC3-I to LC3-II in the cells. Pretreatment with the low dose of MK-8776 suppressed these effects. The above results suggest that MK-8776 increases human TNBC radiosensitivity by inhibiting irradiation-induced autophagy and that MK-8776 may be a potential agent in the radiosensitization of human TNBC.

Keywords: human triple-negative breast cancer; checkpoint kinase 1; MK-8776; radiosensitivity; autophagy; xenograft tumors

Acta Pharmacologica Sinica (2017) 38: 513–523; doi: 10.1038/aps.2016.136; published online 2 Jan 2017

Introduction

Triple-negative breast cancer (TNBC) is known to be highly invasive^[1]. However, the relationship between radiotherapy effectiveness and radiosensitivity remains controversial with respect to TNBC^[2]. Kyndi *et al* suggested that TNBC is relatively radioresistant^[3], but Alkdulbrim *et al* provided evidence that TNBC is radiosensitive^[4]. We previously conducted a retrospective analysis of TNBC patients treated at the Fudan University Shanghai Cancer Center and found that radiotherapy was effective for TNBC, but this effectiveness was limited^[5,6].

Our study confirmed that the radiosensitivity of oestrogen receptor (ER)-negative breast cancer was significantly lower than that of ER-positive breast cancer. Thus, current radiotherapy modalities have a limited effect on TNBC, and more studies are needed to identify new methods that improve the radiosensitivity of TNBC to improve local control rates. In addition, because of the lack of targeted drugs for TNBC, improving the local control rate of TNBC is especially important for improving the prognoses of TNBC patients^[2].

The ability of cancer cells to repair radiation-induced DNA damage is the most important factor that determines their radiosensitivity^[7]. Radiation damages DNA via the direct ionization, excitation or generation of free radicals. DNA damage blocks cell cycle progression while initiating DNA repair mechanisms, which provides the cell with sufficient time to repair the damage. Radiation kills tumour cells mainly by

These authors contributed equally to this work.

* To whom correspondence should be addressed.

E-mail guoxm1800@163.com (Xiao-mao GUO);

xingxing@yahoo.com (Xing-xing CHEN)

Received 2016-08-30 Accepted 2016-11-07

generating unrepaired DNA double-strand breaks (DSBs)^[8]. Thus, targeting DNA damage repair is an effective means of radiosensitization. DNA damage activates cell cycle checkpoints that arrest cell cycle progression and therefore provide time for repair and recovery^[9]. This knowledge has led to the development of checkpoint inhibitors as adjuvants to DNA damaging agents, based on the assumption that they will enhance therapeutic activity. Checkpoint kinase 1 (Chk1) is the primary checkpoint protein against which many small molecule inhibitors have been developed^[10, 11]. Chk1 is activated when the kinases ATM and/or ATR detect double-strand breaks and/or large single-strand regions of DNA, respectively. Once activated, Chk1 phosphorylates and inactivates CDC25 phosphatases that are required for CDK activation and cell cycle progression. Inhibition of Chk1 results in premature activation of CDC25 phosphatases and CDK1/2 and progression through the cell cycle before adequate repair has occurred. Increased DNA damage occurs as affected cells progress through S phase with a damaged template, followed by a lethal mitotic division once they have reached the G₂ phase^[12]. MK-8776 is a recently described inhibitor that is highly selective for Chk1 compared to Chk2 and cyclin-dependent kinases^[10]. Additional studies have shown that MK-8776 enhances the cytotoxicity of hydroxyurea and gemcitabine *in vitro* and *in vivo* without increasing normal tissue toxicities^[10, 13, 14]. However, whether combining MK-8776 with ionizing radiation to treat TNBC is rational remains to be seen. The present study examined the effects of combining MK-8776 with ionizing radiation in human TNBC cell lines and xenografted tumors *in vivo*.

The majority of previous studies have focused on the regulation of autophagy in a variety of models^[15–21]. Our previous data illustrate the importance of IR-induced autophagy and validate autophagic inhibition as a new method of promoting radiosensitivity^[21]. DNA damage repair-related molecules, such as PARP-1, mediate the cytoprotective effects of autophagy in IR-induced tumour cell death, and suppression of autophagy results in IR-induced cell death^[21]. Liu *et al* showed that loss of autophagy leads to decreased levels of Chk1 and a greatly diminished ability to repair DNA double-strand breaks via homologous recombination^[22]. As a result, autophagy-deficient cells are more reliant on nonhomologous end joining (NHEJ) for DNA repair, which enables the use of a unique synthetic strategy of killing cells that may be applicable to the treatment of various forms of human disease.

Based on previous research, enhanced DNA damage repair capacity may be an important mechanism underlying the relative radiation resistance of TNBC cells. Ionizing radiation-induced DNA damage activates Chk1, arresting cell cycle progression and providing time for repair and recovery. However, DNA damage repair-related molecule-mediated autophagy plays a cytoprotective role in IR-induced cancer cell death^[19, 21]. Therefore, we hypothesize that the Chk1 inhibitor MK-8776 increases the radiosensitivity of triple-negative breast cancer by inhibiting autophagy.

Materials and methods

Cell lines and cell culture

The human triple-negative breast cancer cell lines MDA-MB-231 (ATCC[®] HTB-26[™]) and BT-549 (ATCC[®] HTB-122[™]) were purchased from American Type Culture Collection (Manassas, VA, USA), and the CAL-51 breast cancer cell line was purchased from CoBioer Corporation (Nanjing, China). All cell lines were maintained in DMEM supplemented with 10% fetal bovine serum, penicillin (100 units/mL), and streptomycin (100 µg/mL). All cells were incubated at 37°C in a humidified atmosphere with 5.0% CO₂.

Drugs and chemicals

MK-8776, a Chk1 inhibitor, was purchased from Selleck Chemicals (Houston, TX, USA) and dissolved in DMSO. The final DMSO concentration of the solution used throughout the study did not exceed 0.1%. Cells were grown to 70%–80% confluence on plates and treated with different concentration of MK-8776. Before irradiation, the cells were incubated with a low dose of MK-8776 for 1 h to 1.5 h.

Cell cycle detection

Cells were digested at pre-defined time points, and 5.0×10⁵ to 1.0×10⁶ cells were centrifuged at 1500 rounds per minute for 5 min. Then, the cells were washed twice with pre-cooled PBS. The pellet was triturated and mixed well with 100 µL of binding buffer. During vortex, 1 mL of pre-cooled (-20°C) 70% ethanol was added to the mixture, and the cells were fixed in a -20°C freezer for at least two hours. Before staining, the cells were centrifuged at 1500 rounds per minute for 5 min at room temperature. Next, the ethanol was removed, and the cells were washed twice with cold PBS. The supernatant was discarded, and the cells were mixed and resuspended in the residual liquid. Then, 1 mL of propidium iodide (PI) staining solution (50 µg/mL) was added, and kept in the dark at room temperature for 30 min^[2].

Western blotting

Western blotting analysis was performed to determine the expression levels of different proteins in TNBC cells. Cells were harvested, washed with cold 1× PBS, lysed with RIPA lysis buffer (Beyotime, Haimen, China) for 30 min on ice, and then centrifuged at 15000×g for 10 min at 4°C. The total protein concentration was determined using a Bio-Rad protein Assay Kit (Hercules, CA, USA). Equal amounts (20 µg per load) of protein samples were subjected to SDS-PAGE electrophoresis and transferred onto polyvinylidene fluoride (PVDF) membranes (Millipore, Darmstadt, Germany). The blots were blocked in 10% non-fat milk and incubated with primary antibodies, followed by incubation with secondary antibodies conjugated with horseradish peroxidase (HRP). Antibodies to β-Actin and LC3-B were obtained from Sigma-Aldrich (Shanghai, China). Antibodies to Atg5, Chk1, pChk1 (ser345) and pChk1 (ser296) were purchased from Cell Signalling Technology (Danvers, MA, USA). The antibody to γH2A.X was pur-

chased from Abcam (Cambridge, MA, USA). The secondary antibodies were the F(ab)₂ fragment of donkey anti-mouse immunoglobulin (product NA931) or the donkey anti-rabbit immunoglobulin (product NA9340) linked to horseradish peroxidase and were obtained from Amersham Biosciences (Little Chalfont, Buckinghamshire, UK). The immunoblotting reagents were from an electrochemiluminescence kit (Amersham Biosciences).

Immunofluorescence

MK-8776 at concentrations of 100, 200, and 400 nmol/L was incubated with MDA-MB-231, BT-549, or CAL-51 cells for 1 h, and then 8 Gy X-rays were used to irradiate these cells. Two hours later, the cells were fixed with 4% paraformaldehyde. A laser scanning confocal microscope was used to analyse each sample via the same parameters. The numbers of γ H2A.X foci in the nuclei of at least 50 cells were counted in a double-blinded manner to calculate the average number of foci per nucleus.

Cell proliferation

Cells were detached using trypsinization and washed twice with PBS, and 1.0 to 2.0×10^3 cells per well were seeded in 96-well culture plates (Corning Inc, Corning, NY, USA) in 100 μ L medium. The cells were incubated for 12 h to allow attachment, after which a 0-time point measurement was performed. After culturing for 1, 2, 3, 4, and 5 d, the supernatant was removed, and cell growth was assessed using a Cell Counting Kit-8 (CCK-8) assay (Dojindo Laboratories, Kumamoto, Japan), according to the manufacturer's instructions. Absorbance at 450 nm was measured using a microplate reader. The absorbance value is an indicator of cell proliferation and survival: the greater the absorbance value, the greater the survival of the cells. All proliferation assays were performed independently at least 3 times^[2].

Irradiation and colony formation assay

Exponential growth phase cells were irradiated with X-rays (0, 2, 4, 6, and 8 Gy) at 3 Gy/min using a linear accelerator (Varian Medical Systems, Palo Alto, CA, USA) and then digested for counting. The cells were seeded into 60 mm plastic petri dishes, and then the dishes were incubated for 10 to 14 d to allow colonies to develop. The colonies were fixed with 4% paraformaldehyde and stained with 0.1% crystal violet (100% methanol solution) before being counted. The number of clones containing ≥ 50 cells was counted under a stereomicroscope. Plating efficiency (PE) was calculated as follows: $PE = \text{number of colonies formed without irradiation} / \text{number of cells inoculated} \times 100\%$. The cell survival fraction (SF) was calculated at each irradiation dose as follows: $SF = (\text{number of colonies formed at a certain irradiation dose}) / (\text{number of cells inoculated} \times PE)$ ^[2].

In vivo research

A total of 5.0×10^6 to 1.0×10^7 MDA-MB-231 cells suspended in 100 μ L of sterile phosphate-buffered saline (PBS) were

injected subcutaneously into the upper of right hind legs of 48 female BALB/c athymic mice (SLAC Laboratory Animal, Shanghai, China). Tumors were measured every other day; volumes were calculated using the following formula: tumour volume (mm^3) = $a \times b^2 \times 0.5$ (a represents the longest diameter of the tumour, b represents the shortest diameter of the tumour, and 0.5 is an empirical constant). When the tumors reached about 0.5 cm in diameter (approximately 10 d), a total of 48 mice were divided into 6 groups (Vehicle, MK8776 15 mg/kg, MK8776 40 mg/kg, 15 Gy alone, 15 Gy+MK8776 15 mg/kg, 15 Gy+MK8776 40 mg/kg), 8 mice for each group. MK-8776 was administered at a dose of 15 mg/kg ip or 40 mg/kg ip in 2-hydroxypropyl- β -cyclodextrin (45% w/v solution in water) (Sigma-Aldrich, Shanghai, China) at one hour before irradiation. The tumour areas were irradiated with 6 MV X-rays (15 Gy in one fraction) in 3 groups (15 Gy alone, 15 Gy+MK8776 15 mg/kg, 15 Gy+MK8776 40 mg/kg). At 24 h after irradiation, xenograft tumors were harvested from 3 mice in each group and then fixed in formalin to measure γ H2A.X expression (total 18 mice). The rest of mice were followed for approximately 4 weeks and record the size of the xenograft tumors and body weight of mice (total 30 mice). Finally, xenograft tumors were harvested and fixed in formalin. All animal experiments were approved by the Experimental Animal Ethics Committee of Fudan University Shanghai Medical College.

Immunohistochemical staining

Samples from xenograft tumors were fixed using formalin and then used for immunohistochemical staining to measure γ H2A.X expression. Tissues were dehydrated in graded ethanol solutions, cleared in 3 changes of xylene, and penetrated in heated paraffin (56–58 °C). The tissues were embedded in paraffin, cut into 4 to 6 mm sections, and placed onto slides. Before staining, deparaffinization and rehydration were performed. Antigen retrieval was performed using a pressure cooker. The slides were incubated in 1 \times target retrieval solution (Beyotime, Haimen, China) at 120 °C for 4 min at 18 to 20 psi. Endogenous hydrogen peroxidase activity was blocked with hydrogen peroxide for 10 min, followed by rinsing with wash buffer (Beyotime, Haimen, China). The slides were incubated with the appropriate antibodies. The antibodies to γ H2A.X were purchased from Cell Signaling Technology, Inc (Danvers, MA, USA). The secondary antibodies against mouse or rabbit IgG were supplied in an IHC kit from Abcam (Cambridge, MA, USA).

Autophagosome and autophagy detection

Transmission electron microscopy (TEM) performed with an H-600IV microscope (Hitachi, Tokyo, Japan) was utilized to analyse ultra-structural images of autophagic vacuoles, autophagosomes and autolysosomes. The three TNBC cell lines were harvested via trypsinization, washed twice with PBS, and fixed with ice-cold glutaraldehyde (3% in 0.1 mol/L cacodylate buffer, pH=7.4) for 24 h. The cells were post fixed in OsO₄, dehydrated in a graded series of 70% to 100% acetone, and then embedded in Epon 812. One micrometre sections were

cut, double stained with uranium tetraacetate and lead citrate trihydrate, and viewed using transmission electron microscopy with scanning attachments. A StubRFP-SensGFP-LC3 lentivirus (Genechem, Shanghai, China) was used to infect MDA-MB-231 cells and to facilitate the detection of autophagy. The red fluorescent protein Stub-RFP, the green fluorescent protein Sens-GFP and the autophagy marker protein LC3 were assembled into protein complexes. At the beginning of autophagy, these Stub-RFP-Sens-GFP complexes surrounded autophagosomes, and red/green fluorescent dots were observed via microscopy. Late in autophagy, lysosomes and autophagosomes fused into autolysosomes when $\text{pH}<5$, and the absence of Sens-GFP fluorescence indicated that only red fluorescent dots were present. This procedure was performed in accordance with the manufacturer's instructions (Genechem, Shanghai, China).

Statistical analysis

Results were expressed as the mean \pm standard deviation (SD) or the mean \pm standard error (SEM). Comparisons between multiple groups were conducted using one-way ANOVA or two-way ANOVA for quantitative data. *Post hoc* analyses were performed using the LSD *t*-test. Statistical analysis was performed using SPSS Statistics 22.0 (IBM SPSS, NY, USA) and GraphPad Prism 6.0 (GraphPad Software Inc, San Diego, CA, USA). *P* values less than 0.05 were considered statistically significant. Survival fraction curve fitting was conducted with the linear-quadratic model^[23] via the equation $y=\exp[-(a\times x+b\times x^2)]$.

Results

The Chk1 inhibitor MK-8776 abrogates ionizing radiation-induced cell cycle arrest

We determined the IC_{50} of MK-8776 in the above mentioned three TNBC cell lines. In MDA-MB-231, BT-549 and CAL-51 cells, the IC_{50} s of MK8776 were 9.403, 17.60, and 2.102 $\mu\text{mol/L}$, respectively (Figure 1A–1C). Based on the results of our preliminary experiment and the above IC_{50} values, we chose MK-8776 at concentrations of 100, 200, and 400 nmol/L to treat the MDA-MB-231, BT-549, or CAL-51 cell lines. Then, we performed cell cycle detection at 4, 8, 24, and 36 h after irradiation at a dose of 6 Gy. The results showed that MK-8776 abrogates ionizing radiation-induced cell cycle arrest at 24 h after irradiation in the three TNBC cell lines. Compared with ionizing radiation (IR) alone, the combination of IR+MK-8776 significantly decreased the proportions of MDA-MB-231 (0.22 ± 0.011 vs 0.318 ± 0.034 , $P=0.011$), BT-549 (0.363 ± 0.011 vs 0.304 ± 0.028 , $P=0.027$) and CAL-51 (0.336 ± 0.022 vs 0.251 ± 0.021 , $P=0.009$) cells in G_2/M phase at 24 h after irradiation, as shown in Figure 1D–1F. CAL51 cell line showed a decreased G_2/M to 36 h in the IR+MK-8776 group (Figure 1F).

MK-8776 enhances ionizing radiation-induced DNA damage

We performed immunofluorescence assays and counted the numbers of $\gamma\text{H2A.X}$ foci in the nuclei of at least 50 cells to calculate the average numbers of foci per nucleus and the

percentages of nuclei with more than 10 foci among the three types of TNBC cells. Compared with the untreated group, the groups that received ionizing radiation or IR+MK-8776 exhibited significantly increased percentages of nuclei with more than 10 foci in the three TNBC cell lines (Figure 2A–2D). In addition, compared with IR alone, IR+MK-8776 also significantly increased the percentages of nuclei with more than 10 foci in the MDA-MB-231 ($39.67\pm 3.51\%$ vs $33.0\pm 2\%$, $P=0.046$), BT-549 ($51.67\pm 3.06\%$ vs $35.33\pm 1.33\%$, $P=0.001$) and CAL-51 ($39.33\pm 2.52\%$ vs $32\pm 3.61\%$, $P=0.045$) cell lines, as shown in Figure 2A–2D. Furthermore, we used Western blotting to measure the levels of Chk1 phosphorylation at ser345 and ser296, of total Chk1 and of $\gamma\text{H2A.X}$ at 2 h after irradiation. We noted markedly increased phosphorylation of Chk1 at ser296 after irradiation, which was inhibited by MK-8776, as shown in Figure 2E. In contrast, we detected no Chk1 phosphorylation at ser345 after irradiation, as shown in Figure 2E. We noted a dramatic increase in $\gamma\text{H2A.X}$ after irradiation with or without MK-8776. Compared with ionizing radiation alone, IR+MK-8776 significantly increased the phosphorylation of H2A.X, which suggests that MK-8776 enhances ionizing radiation-induced DNA damage, as shown in Figure 2E.

MK-8776 inhibits TNBC cell proliferation and increases the radiosensitivity of breast cancer *in vitro*

We performed cell proliferation analysis and cell colony formation assay to determine whether MK-8776 increases the radiosensitivity of TNBC. The results of the cell proliferation assay showed that the cell viability rate of TNBC cells treated with the combination of MK-8776 and 6 Gy X-rays was significantly lower than that of TNBC cells treated with 6 Gy alone in all three TNBC cell lines, suggesting that MK-8776 can inhibit TNBC cell proliferation and increase TNBC radiosensitivity, as shown in Figure 3A–3C. Similar results were obtained via the cell colony formation assay, indicating that MK-8776 contributes to the radiation sensitization of three types of TNBC cell lines *in vitro*. GraphPad Prism 6.0 software was used to calculate radiobiology parameters and survival fraction curves via the linear-quadratic model; the results are shown in Figure 3D–3F. Furthermore, Figure 3G shows a comparison of the numbers of clones at 14 d after irradiation in MDA-MB-231 cells treated with and without MK-8776. All these results showed that compared with irradiation alone, the combination of MK-8776 and irradiation significantly increased the radiosensitivity of the three TNBC cell lines *in vitro*.

MK-8776 increases the radiosensitivity of breast cancer *in vivo*

To determine the synergistic sensitization effects of MK-8776 *in vivo*, we inoculated MDA-MB-231 cells into the upper right hind legs of nude mice with or without MK-8776 treatment at concentrations of 15 or 40 mg/kg ($n=8$ mice for each group, total 48 mice). As shown in Figure 4A–4D, at 26 d after irradiation, compared with the groups treated with irradiation alone or MK-8776 alone, the volumes (mm^3) of the xenograft tumors were significantly decreased in the groups treated

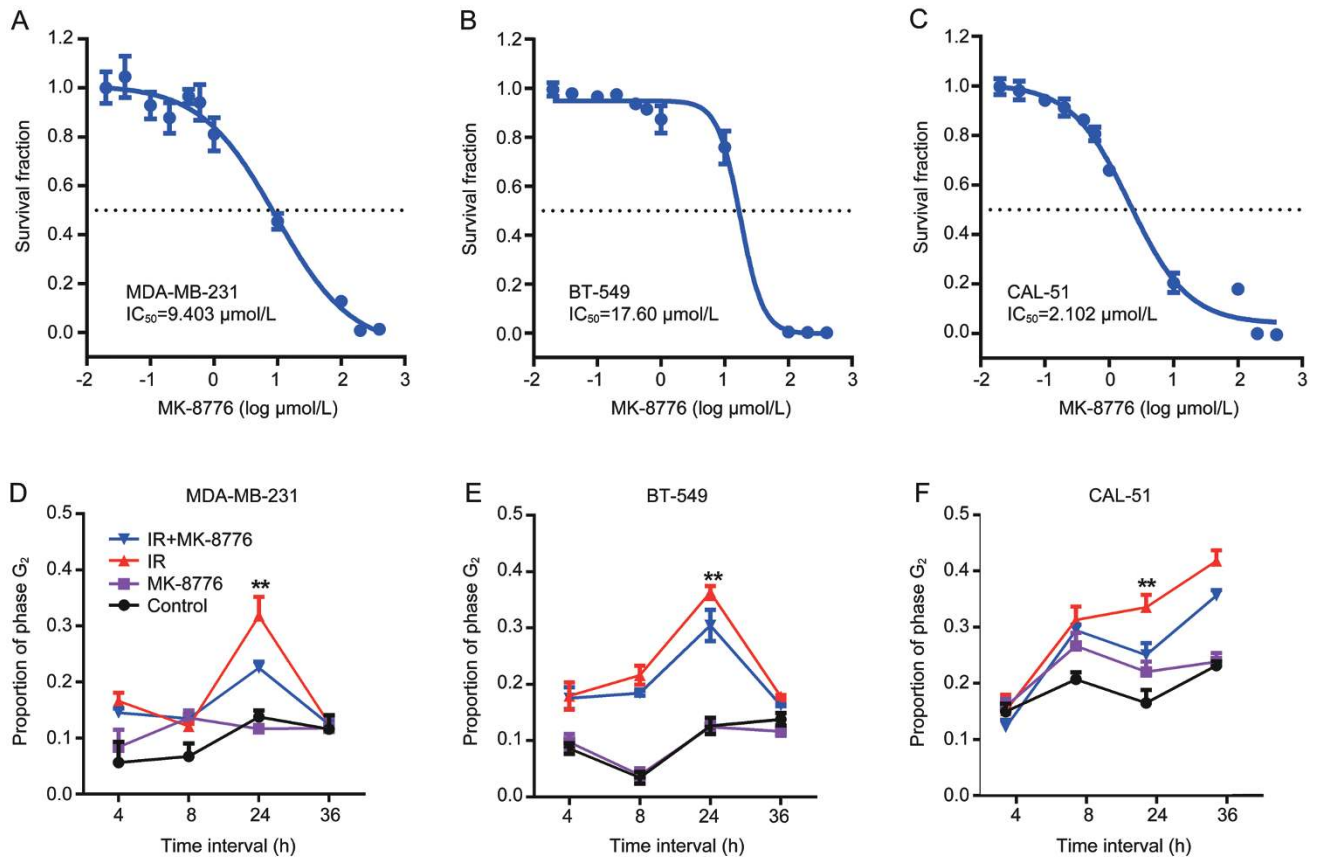


Figure 1. MK-8776 abrogates irradiation-induced cell cycle arrest. (A) IC_{50} of MK-8776 in MDA-MB-231 cells; (B) IC_{50} of MK-8776 in BT-549 cells; (C) IC_{50} of MK8776 in CAL-51 cells. (D–F) Cell cycle detection at 4, 8, 24, and 36 h after the combination of irradiation at a dose of 6 Gy and MK-8776 at concentrations of 100 nmol/L, 200 nmol/L and 400 nmol/L was used to treat the three TNBC cell lines, respectively. Compared with ionizing radiation (IR) alone, 24 h after irradiation, IR+MK-8776 significantly decreased the proportions of cells in G₂/M phase in the MDA-MB-231 (0.22 ± 0.011 vs 0.318 ± 0.034 , $P=0.011$) (D), BT-549 (0.363 ± 0.011 vs 0.304 ± 0.028 , $P=0.027$) (E) and CAL-51 cell lines (0.336 ± 0.022 vs 0.251 ± 0.021 , $P=0.009$) (F). Error bars represent SDs. ** $P < 0.05$.

with MK-8776 combined with irradiation at either 15 mg/kg MK-8776+15 Gy group or 40 mg/kg MK-8776+15 Gy group (Vehicle vs 15 Gy+MK8776 15 mg/kg vs MK8776 15 mg/kg vs MK8776 40 mg/kg vs 15 Gy alone vs 15 Gy+MK8776 40 mg/kg; $2317.87 \pm 62.08 \text{ mm}^3$ vs $431.94 \pm 120.18 \text{ mm}^3$ vs $1263.57 \pm 309.82 \text{ mm}^3$ vs $1102.34 \pm 144.30 \text{ mm}^3$ vs $887.10 \pm 164.53 \text{ mm}^3$ vs $407.82 \pm 75.54 \text{ mm}^3$, respectively, $P < 0.0001$). However, there were no differences in volume between the 15 mg/kg MK-8776+IR group and 40 mg/kg MK-8776+IR group ($431.94 \pm 120.18 \text{ mm}^3$ vs $407.82 \pm 75.54 \text{ mm}^3$, $P=0.87$), as shown in Figure 4A. To determine whether MK-8776 affects the expression of $\gamma\text{H2A.X}$ *in vivo*, we performed IHC analysis on tumour sections from all the experimental groups. Xenograft tumors were randomly harvested from 3 nude mice in each group at 24 h after irradiation and then fixed in formalin to measure $\gamma\text{H2A.X}$ expression. As shown in Figure 4E, the MK-8776+IR group exhibited significantly increased $\gamma\text{H2A.X}$ expression compared with the untreated, MK-8776-alone and IR-alone groups, suggesting that MK-8776 enhances ionizing radiation-induced DNA damage *in vivo* and consequently increases

the radiosensitivity of breast cancer *in vivo*.

MK-8776 increases the radiosensitivity of TNBC by inhibiting autophagy

We studied the mechanisms underlying the synergistic sensitization effects of MK-8776 in the treatment of TNBC. Based on the results of a previous study, we assumed that MK-8776 inhibits cell autophagy induced by radiation and that autophagy itself protects tumour cells against irradiation. When this protective mechanism is inhibited, tumour cell sensitivity to irradiation increases. We used a StubRFP-SensGFP-LC3 lentivirus to infect the three TNBC cell lines and to detect autophagy flow. Before irradiation, all TNBC cells were treated with MK-8776 for 1 h, and the cells were then irradiated at a dose of 8 Gy. Twenty-four hours later, the cells were observed via confocal fluorescence microscopy. As shown in Figure 5A, 5B, MK-8776 inhibited irradiation-induced cell autophagy. Among the three TNBC cell lines, the numbers of autophagy-related fluorescent spots were significantly increased in the IR-alone group, and these effects were signif-

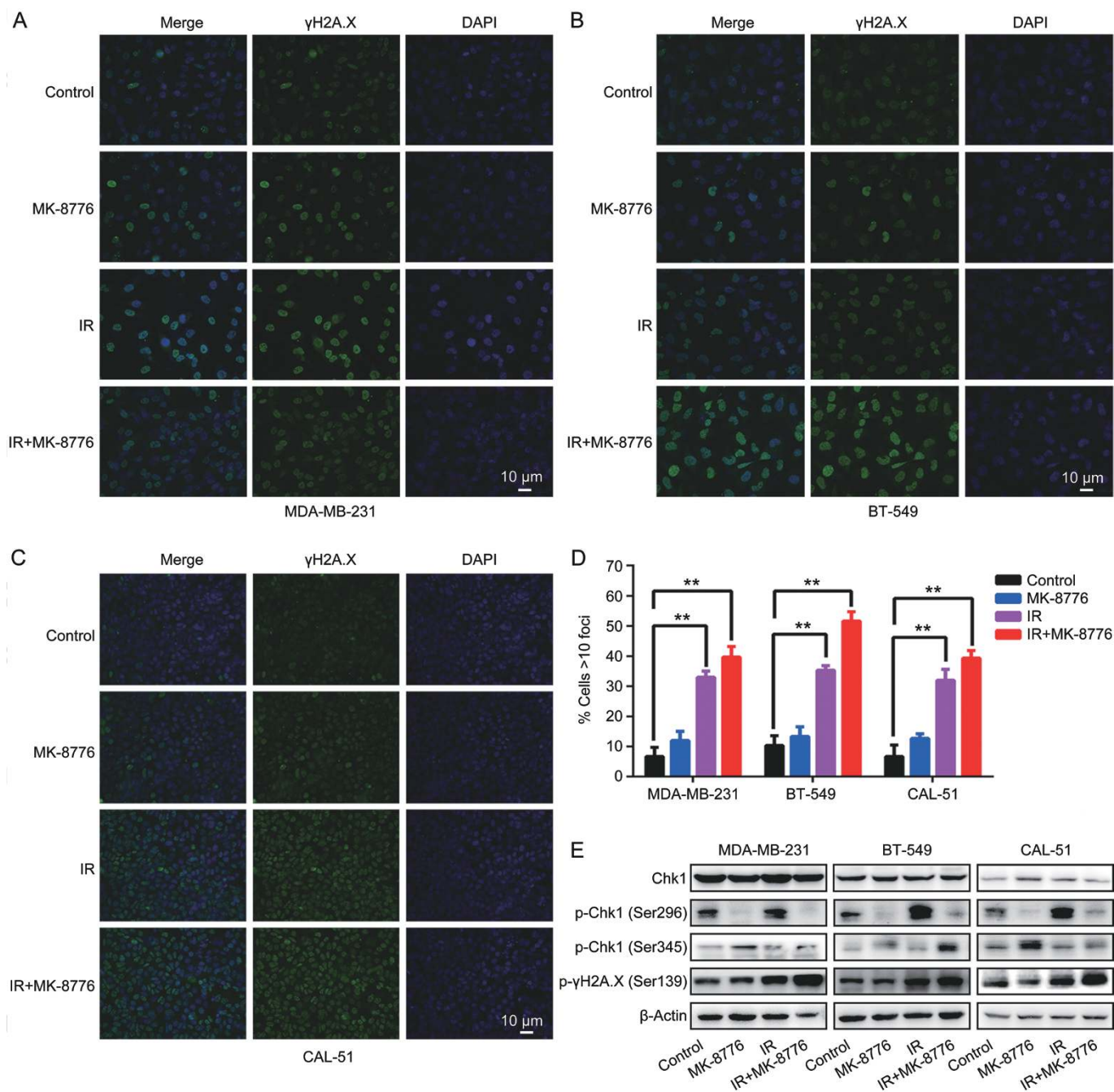


Figure 2. MK-8776 enhances irradiation-induced DNA damage. (A–C) Immunofluorescence assay results and the numbers of γ H2A.X foci in the three TNBC cell types; (D) Compared with the IR-alone group, the IR+MK-8776 group also exhibited significantly increased percentages of more than 10 foci in the MDA-MB-231 ($39.67\% \pm 3.51\%$ vs $33.0\% \pm 2\%$, $P=0.046$), BT-549 ($51.67\% \pm 3.06\%$ vs $35.33\% \pm 1.33\%$, $P=0.001$) and CAL-51 ($39.33\% \pm 2.52\%$ vs $32\% \pm 3.61$, $P=0.045$) cell lines. (E) Markedly increased phosphorylation of Chk1 at ser296 was observed after irradiation, which was inhibited by MK-8776. No detectable phosphorylation of Chk1 at ser345 was observed after irradiation. A dramatic increase in γ H2A.X was observed after irradiation with or without MK-8776. Error bars represent SDs. $**P<0.05$.

icantly suppressed by MK-8776 (IR vs MK-8776+IR: 65 ± 23 vs 13 ± 8 , $P<0.0001$ in MDA-MB-231; 57 ± 32 vs 18 ± 7 , $P=0.0014$ in BT-549; 43 ± 35 vs 14 ± 10 , $P=0.021$ in CAL-51), as shown in Figure 5A, 5B. We used TEM to detect autophagy and counted the numbers of autophagosomes or autophagic vacuoles. Before irradiation, the cells were treated with MK-8776 for

1.5 h and then irradiated at dose of 8 Gy. Forty-eight hours later, the cells were harvested and fixed with glutaraldehyde. Similar results were observed in the three TNBC cell lines, as shown in Figure 5C–5D. MK-8776 significantly decreased the levels of irradiation-induced autophagy (IR vs MK-8776+IR: 35 ± 12 vs 13 ± 5 , $P<0.0001$ in MDA-MB-231; 40 ± 15 vs 16 ± 4 ,

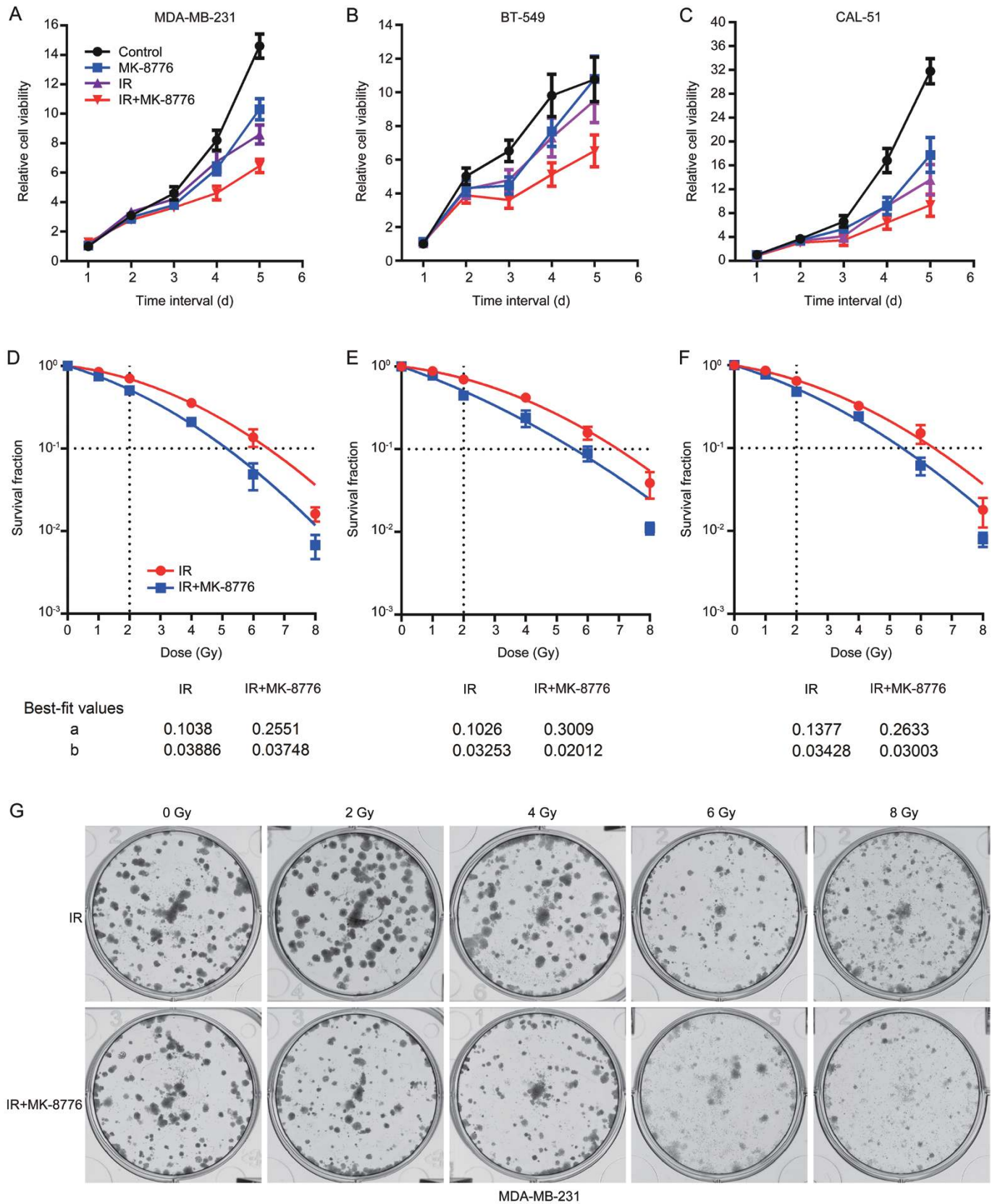


Figure 3. MK-8775 inhibits cell proliferation and increases the radiosensitivity of breast cancer *in vitro*. (A–C) Cell proliferation assay showed that the cell viability rates of cells treated with MK-8776 combined with 6 Gy X-rays were significantly lower than those of cells treated with irradiation alone in the three types of TNBC cells; (D–F) Survival fraction curves showed that MK-8776 combined with irradiation significantly increased the radiosensitivity of the three TNBC cell lines. (G) Numbers of clones at 14 d after irradiation in MDA-MB-231 cells treated with and without MK-8776.

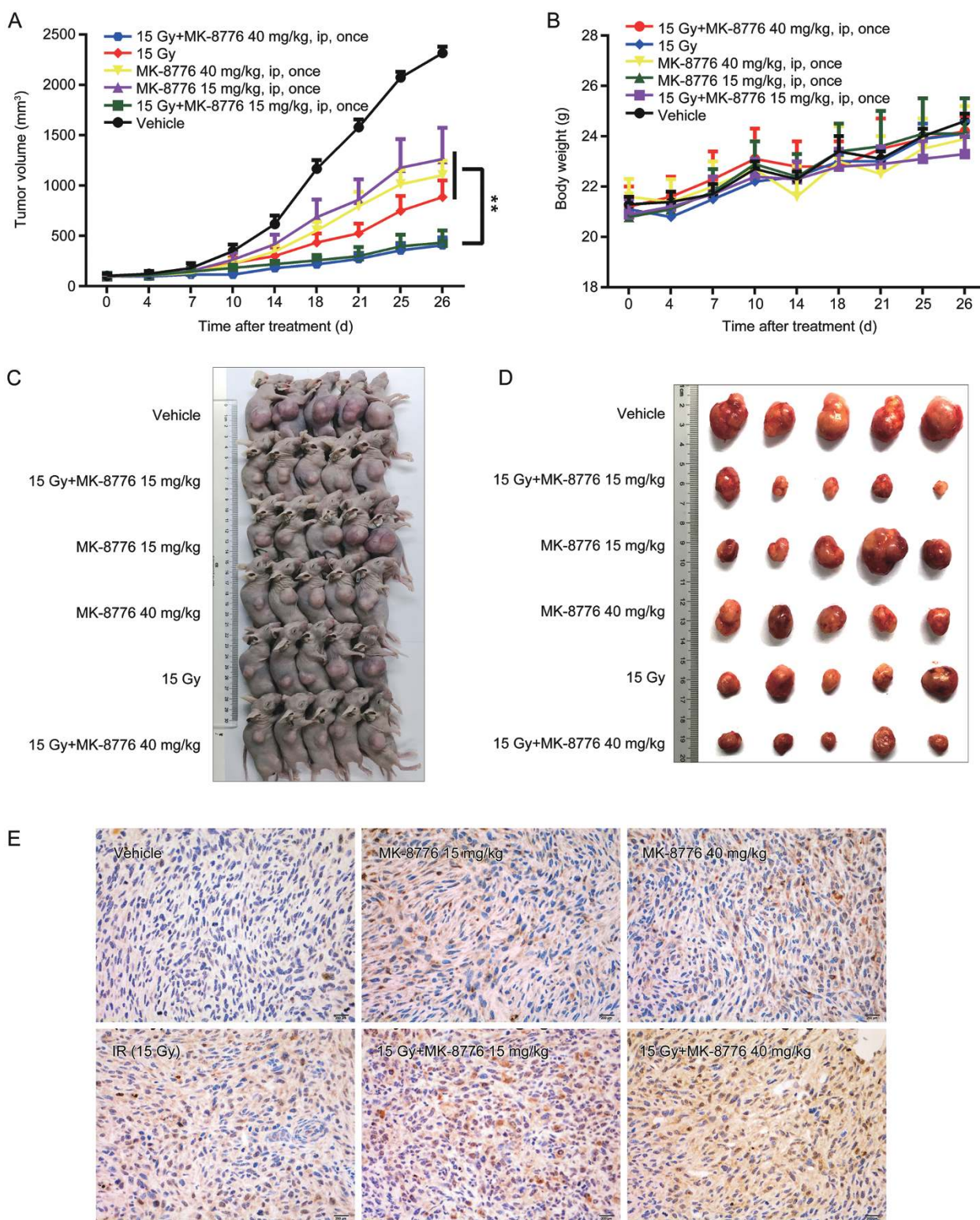


Figure 4. MK-8775 increased the radiosensitivity of breast cancer *in vivo*. (A, C, D) At 26 d after irradiation, compared with the irradiation-alone group or MK-8776-alone group, the volumes (mm^3) of the xenograft tumors were significantly decreased in the group treated with MK-8776 combined with irradiation [Vehicle vs (15 Gy+MK8776 15 mg/kg) vs (MK8776 15 mg/kg) vs (MK8776 40 mg/kg) vs (15 Gy alone) vs (15 Gy+MK8776 40 mg/kg): $2317.87 \pm 62.08 \text{ mm}^3$ vs $431.94 \pm 120.18 \text{ mm}^3$ vs $1263.57 \pm 309.82 \text{ mm}^3$ vs $1102.34 \pm 144.30 \text{ mm}^3$ vs $887.10 \pm 164.53 \text{ mm}^3$ vs $407.82 \pm 75.54 \text{ mm}^3$, respectively, $P < 0.0001$]. There were no differences in volume between the 15 mg/kg MK-8776+IR group and 40 mg/kg MK-8776+IR group ($431.94 \pm 120.18 \text{ mm}^3$ vs $407.82 \pm 75.54 \text{ mm}^3$, $P = 0.87$); (B) There were no difference on body weight of nude mice among different treatment groups; (E) MK-8776+IR significantly increased the expression of $\gamma\text{H2A.X}$ compared with the untreated, MK-8776-alone and IR-alone groups. Error bars represent SEMs. $**P < 0.05$.

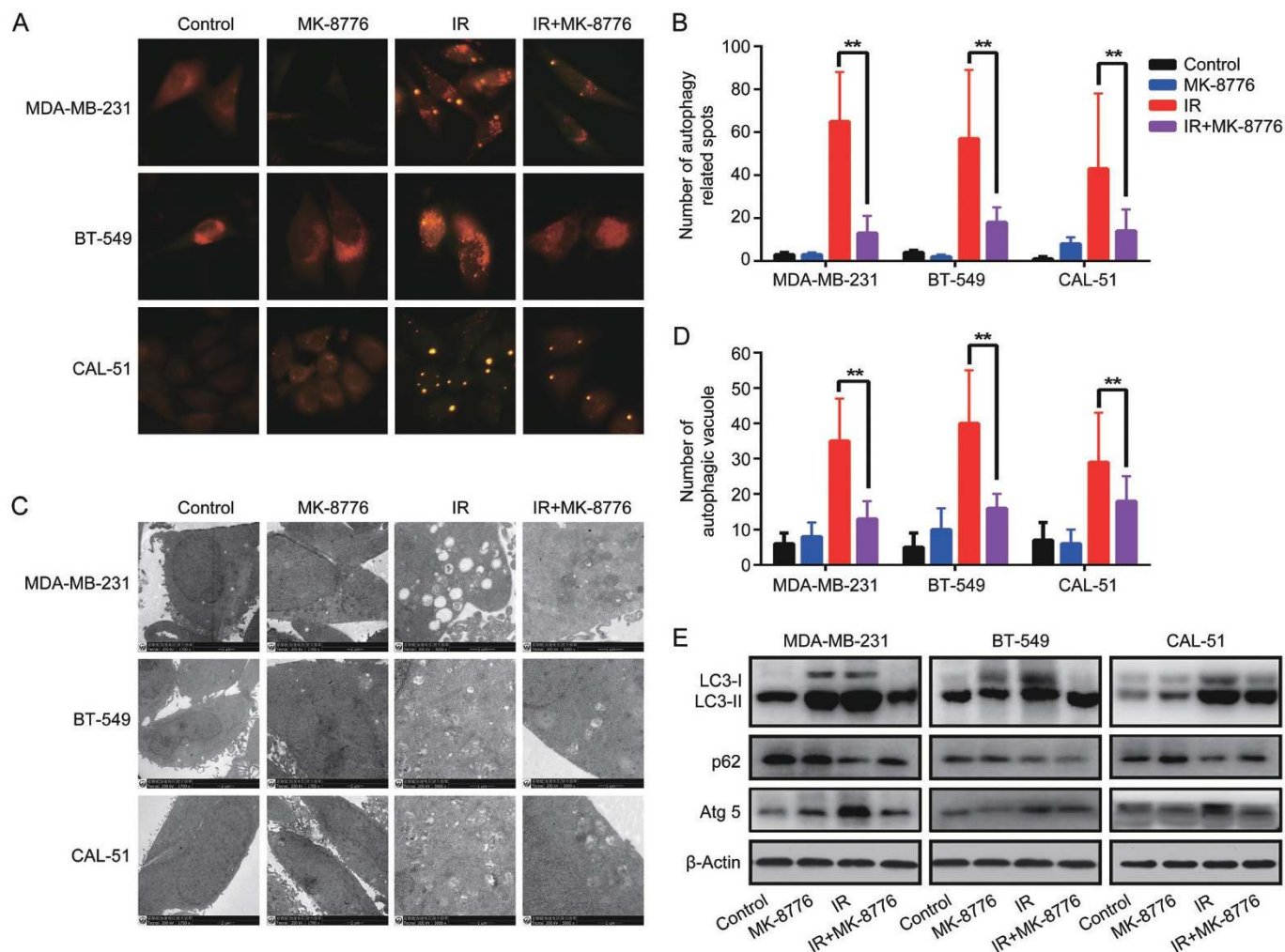


Figure 5. MK-8776 increases the radiosensitivity of TNBC by inhibiting autophagy. (A, B) In the three TNBC cell lines, the numbers of autophagy-related spots were significantly increased in IR-alone group, and this effect was significantly suppressed by MK-8776 (IR vs MK-8776+IR: 65 ± 23 vs 13 ± 8 , $P < 0.0001$ in MDA-MB-231; 57 ± 32 vs 18 ± 7 , $P = 0.0014$ in BT-549; 43 ± 35 vs 14 ± 10 , $P = 0.021$ in CAL-51). (C, D) MK-8776 significantly decreased the numbers of irradiation-induced autophagosomes (IR vs MK-8776+IR: 35 ± 12 vs 13 ± 5 , $P < 0.0001$ in MDA-MB-231; 40 ± 15 vs 16 ± 4 , $P = 0.0001$ in BT-549; 29 ± 14 vs 18 ± 7 , $P = 0.039$ in CAL-51). (E) Irradiation increased the levels of Atg5 and promoted the transformation of LC3-I to LC3-II; these effects were inhibited by MK-8776. Contrasting results were observed regarding p62 expression. Error bars represent SDs. ** $P < 0.05$.

$P = 0.0001$ in BT-549; 29 ± 14 vs 18 ± 7 , $P = 0.039$ in CAL-51). We used Western blotting to determine the expression levels of autophagy-related proteins. Irradiation increased the level of Atg5 and promoted the transformation of LC3-I to LC3-II. These effects were inhibited by MK-8776. Contrasting results were observed regarding p62 expression, as shown in Figure 5E. All these results suggest that MK-8776 inhibits radiation-induced autophagy and increases the radiosensitivity of TNBC.

Discussion

Thus far, several specific Chk1 inhibitors have been developed to treat different cancers. Two of them, MK-8776 and Prexasertib, have reached phase I/II clinical trials and shown acceptable safety and pharmacokinetic profiles^[11, 24, 25]. However, Chk1 inhibitors are being developed only as chemotherapy

potentiators or single-agent therapies^[25], Montano *et al* found that MK-8776 markedly sensitizes multiple cell lines to gemcitabine^[14]. Wang *et al* found that the anticancer properties of LY2603618 may be enhanced by an autophagy inhibitor^[26]. Schenk *et al* concluded that a selective Chk1 inhibitor can overcome the S phase checkpoint and enhance the cytotoxicity of cytarabine^[13]. To our knowledge, there are no studies investigating MK-8776 as a radiotherapy sensitizer. Thus, we performed this study to evaluate its radiotherapy sensitization effects in TNBC and to investigate the underlying cellular mechanisms of these effects *in vitro* and *in vivo*. The results of our research indicated that MK-8776 sensitized three TNBC cell types (MDA-MB-231, BT-549, and CAL-51) to ionizing radiation, possibly by abrogating G₂/M arrest, enhancing the inhibition of post-irradiation cell proliferation, increasing double-strand breaks (DSBs) damage and inhibiting irradiation-

tion-induced autophagy. MK-8776 may exert its effects via autophagy inhibition.

Cell cycle arrest induced by DNA damage occurs via the cascade reaction of ATM/ATR-Chk1/Chk2-Cdc25A/Cdc25C, which eventually results in the inhibitory phosphorylation of Cdc2 and activation of the cyclinB1/Cdc2 complex^[27, 28]. Chk1 is phosphorylated mainly at Ser345 and Ser296 in response to DNA damage^[26, 29]. Ser345 phosphorylation is predominantly catalysed by ATR, while Ser296 phosphorylation occurs via autophosphorylation^[26]. The results of our study showed that MK-8776 inhibited irradiation-induced Ser296 Chk1 phosphorylation in TNBC cells. However, the levels of irradiation-induced Ser-345 Chk1 (pSer345 Chk1) phosphorylation increased significantly in response to low doses of MK-8776 (100 nmol/L, 200 nmol/L and 400 nmol/L) (Figure 2E), indicating that MK-8776 induces DNA damage responses and further amplifies ATR/ATM-mediated Chk1 phosphorylation (Ser296) in TNBC cells. These results are consistent with those of a study by Montano *et al*, in which the Chk1 inhibitor MK-8776 also inhibited DNA damaging agent and antimetabolite-induced Chk1 (Ser296) phosphorylation^[11, 26]. Guzi and Schenket's studies reported similar results, as both found that MK-8776 decreased cytarabine- and hydroxyurea-induced Chk1 (Ser296) phosphorylation but not Chk1 (Ser345) phosphorylation^[10, 13].

When cancer cells are exposed to DNA damage-inducing chemotherapeutic agents or ionizing irradiation, double-strand breaks (DSBs) are subsequently generated^[30], rapidly resulting in H2A.X phosphorylation at Ser139 (γ H2A.X) by ATM, ATR or the DNA-PK pathway^[26, 31]. Because this process is very robust and fast and is strongly associated with DSBs, H2A.X phosphorylation is considered a sensitive marker of DNA damage^[26, 31]. In this study, irrespective of the cellular immunofluorescence detection method, our results showed that MK-8776 significantly increased the expression of phosphorylated γ H2A.X, suggesting that MK-8776 significantly increases irradiation-induced DNA damage responses in TNBC cells and that these results were very robust (Figure 2A–2E and Figure 4D). In previous studies, similar results were reported regarding multiple chemotherapeutic agents and irradiation, which impacted DNA replication and elicited the accumulation of γ H2A.X when combined with MK-8776^[10, 11, 13, 26, 31, 32], suggesting that MK-8776 is a DNA damage enhancer.

We hypothesized that the Chk1 inhibitor MK-8776 increases the radiosensitivity of TNBC by inhibiting autophagy. Thus, we detected autophagy in TNBC cells using TEM, a StubRFP-SensGFP-LC3 lentivirus and Western blotting. Our results showed that irradiation can cause significant autophagic changes and increase LC3-II protein levels in TNBC cells. LC3-II is currently the only known protein located on autophagosomes and autophagosome-lysosome membranes^[21, 33]. When TNBC cells were pretreated with MK-8776 *in vitro*, the results showed that autophagy was markedly decreased (Figure 5). We also measured the levels of other autophagy-related proteins, such as Atg5, and observed similar findings. MK-8776 inhibited irradiation-induced increases in Atg5

expression. Contrasting results were observed regarding p62 expression. Therefore, all these results supported our hypothesis. To our knowledge, there are few studies regarding the relationship among MK-8776, radiosensitivity and autophagy, although several studies have investigated the relationship between Chk1 inhibitors and autophagy. Park and his colleagues found that nuclear accumulation of Chk1 in chaperone-mediated autophagy-deficient cells compromises the cell cycle and prolongs DNA damage in affected cells^[34]. Liu *et al* reported that autophagy inhibition caused elevated proteasome activity, leading to enhanced degradation of Chk1^[22]. Wang *et al* found that inhibiting autophagy may enhance the anticancer properties of LY2603618 (another Chk1 inhibitor)^[26]. Because the main purpose of this study was to explore the radiotherapy sensitization effects of MK-8776, we did not sufficiently explore the relationship between MK-8776 and autophagy. In the future, we will reversibly inhibit autophagy or use autophagy-deficient cells to investigate the relationship between autophagy and the radiotherapy sensitization effects of MK-8776.

In conclusion, our results show that the Chk1 inhibitor MK-8776 increases the radiosensitivity of three triple-negative breast cancer cell lines by inhibiting autophagy *in vitro*. MK-8776 may have potential as a radiotherapy sensitization agent. More involved and comprehensive studies may be needed to determine the correlation between MK-8776 and cell autophagy.

Acknowledgements

This work was partly supported by the National Natural Science Foundation of China (Grant No 81072164, 81372430, and 81402525) and the Shanghai Sailing Program (Grant No 16YF1401700). The authors thank Eunice XU (AME Publishing Company, Guangzhou, China) for proofreading the manuscript.

Author contribution

Conception and design: Xiao-mao GUO and Xing-xing CHEN; Collection and assembly of the data: Zhi-rui ZHOU and Zhao-zhi YANG; Data analysis and interpretation: Zhi-rui ZHOU, Xiao-mao GUO, and Xiao-li YU; Manuscript writing: all authors; Final approval of the manuscript: all authors; Financial support: Xiao-li YU, Xing-xing CHEN, and Xiao-mao GUO.

References

- 1 Jiao Q, Wu A, Shao G, Peng H, Wang M, Ji S, *et al*. The latest progress in research on triple negative breast cancer (TNBC): risk factors, possible therapeutic targets and prognostic markers. *J Thorac Dis* 2014; 6: 1329–35.
- 2 Hou J, Zhou Z, Chen X, Zhao R, Yang Z, Wei N, *et al*. HER2 reduces breast cancer radiosensitivity by activating focal adhesion kinase *in vitro* and *in vivo*. *Oncotarget* 2016; 7: 45186–98.
- 3 Kyndi M, Sorensen FB, Knudsen H, Overgaard M, Nielsen HM, Overgaard J. Estrogen receptor, progesterone receptor, HER-2, and response to postmastectomy radiotherapy in high-risk breast cancer: the Danish Breast Cancer Cooperative Group. *J Clin Oncol* 2008; 26:

- 1419–26.
- 4 Efimova EV, Mauceri HJ, Golden DW, Labay E, Bindokas VP, Darga TE, *et al*. Poly(ADP-ribose) polymerase inhibitor induces accelerated senescence in irradiated breast cancer cells and tumors. *Cancer Res* 2010; 70: 6277–82.
 - 5 Chen X, Yu X, Chen J, Yang Z, Shao Z, Zhang Z, *et al*. Radiotherapy can improve the disease-free survival rate in triple-negative breast cancer patients with T1–T2 disease and one to three positive lymph nodes after mastectomy. *Oncologist* 2013; 18: 141–7.
 - 6 Chen X, Yu X, Chen J, Zhang Z, Tuan J, Shao Z, *et al*. Analysis in early stage triple-negative breast cancer treated with mastectomy without adjuvant radiotherapy: patterns of failure and prognostic factors. *Cancer* 2013; 119: 2366–74.
 - 7 Chalmers AJ, Lakshman M, Chan N, Bristow RG. Poly(ADP-ribose) polymerase inhibition as a model for synthetic lethality in developing radiation oncology targets. *Semin Radiat Oncol* 2010; 20: 274–81.
 - 8 Ashworth A. A synthetic lethal therapeutic approach: poly(ADP) ribose polymerase inhibitors for the treatment of cancers deficient in DNA double-strand break repair. *J Clin Oncol* 2008; 26: 3785–90.
 - 9 Reinhardt HC, Hasskamp P, Schmedding I, Morandell S, van Vugt MA, Wang X, *et al*. DNA damage activates a spatially distinct late cytoplasmic cell-cycle checkpoint network controlled by MK2-mediated RNA stabilization. *Mol Cell* 2010; 40: 34–49.
 - 10 Guzi TJ, Paruch K, Dwyer MP, Labroli M, Shanahan F, Davis N, *et al*. Targeting the replication checkpoint using SCH 900776, a potent and functionally selective CHK1 inhibitor identified via high content screening. *Mol Cancer Ther* 2011; 10: 591–602.
 - 11 Montano R, Chung I, Garner KM, Parry D, Eastman A. Preclinical development of the novel Chk1 inhibitor SCH900776 in combination with DNA-damaging agents and antimetabolites. *Mol Cancer Ther* 2012; 11: 427–38.
 - 12 Kohn EA, Ruth ND, Brown MK, Livingstone M, Eastman A. Abrogation of the S phase DNA damage checkpoint results in S phase progression or premature mitosis depending on the concentration of 7-hydroxystaurosporine and the kinetics of Cdc25C activation. *J Biol Chem* 2002; 277: 26553–64.
 - 13 Schenk EL, Koh BD, Flatten KS, Peterson KL, Parry D, Hess AD, *et al*. Effects of selective checkpoint kinase 1 inhibition on cytarabine cytotoxicity in acute myelogenous leukemia cells *in vitro*. *Clin Cancer Res* 2012; 18: 5364–73.
 - 14 Montano R, Thompson R, Chung I, Hou H, Khan N, Eastman A. Sensitization of human cancer cells to gemcitabine by the Chk1 inhibitor MK-8776: cell cycle perturbation and impact of administration schedule *in vitro* and *in vivo*. *BMC Cancer* 2013; 13: 604.
 - 15 Komatsu M, Waguri S, Chiba T, Murata S, Iwata J, Tanida I, *et al*. Loss of autophagy in the central nervous system causes neurodegeneration in mice. *Nature* 2006; 441: 880–4.
 - 16 Apel A, Herr I, Schwarz H, Rodemann HP, Mayer A. Blocked autophagy sensitizes resistant carcinoma cells to radiation therapy. *Cancer Res* 2008; 68: 1485–94.
 - 17 Cao C, Subhawong T, Albert JM, Kim KW, Geng L, Sekhar KR, *et al*. Inhibition of mammalian target of rapamycin or apoptotic pathway induces autophagy and radiosensitizes PTEN null prostate cancer cells. *Cancer Res* 2006; 66: 10040–7.
 - 18 Lomonaco SL, Finniss S, Xiang C, Decarvalho A, Umansky F, Kalkanis SN, *et al*. The induction of autophagy by gamma-radiation contributes to the radioresistance of glioma stem cells. *Int J Cancer* 2009; 125: 717–22.
 - 19 Paglin S, Lee NY, Nakar C, Fitzgerald M, Plotkin J, Deuel B, *et al*. Rapamycin-sensitive pathway regulates mitochondrial membrane potential, autophagy, and survival in irradiated MCF-7 cells. *Cancer Res* 2005; 65: 11061–70.
 - 20 Peng PL, Kuo WH, Tseng HC, Chou FP. Synergistic tumor-killing effect of radiation and berberine combined treatment in lung cancer: the contribution of autophagic cell death. *Int J Radiat Oncol Biol Phys* 2008; 70: 529–42.
 - 21 Zhou ZR, Zhu XD, Zhao W, Qu S, Su F, Huang ST, *et al*. Poly(ADP-ribose) polymerase-1 regulates the mechanism of irradiation-induced CNE-2 human nasopharyngeal carcinoma cell autophagy and inhibition of autophagy contributes to the radiation sensitization of CNE-2 cells. *Oncol Rep* 2013; 29: 2498–506.
 - 22 Liu EY, Xu N, O'Prey J, Lao LY, Joshi S, Long JS, *et al*. Loss of autophagy causes a synthetic lethal deficiency in DNA repair. *Proc Natl Acad Sci U S A* 2015; 112: 773–8.
 - 23 Jones L, Hoban P, Metcalfe P. The use of the linear quadratic model in radiotherapy: a review. *Australas Phys Eng Sci Med* 2001; 24: 132–46.
 - 24 Thompson R, Eastman A. The cancer therapeutic potential of Chk1 inhibitors: how mechanistic studies impact on clinical trial design. *Br J Clin Pharmacol* 2013; 76: 358–69.
 - 25 McNeely S, Beckmann R, Bence Lin AK. CHEK again: revisiting the development of CHK1 inhibitors for cancer therapy. *Pharmacol Ther* 2014; 142: 1–10.
 - 26 Wang FZ, Fei HR, Cui YJ, Sun YK, Li ZM, Wang XY, *et al*. The checkpoint 1 kinase inhibitor LY2603618 induces cell cycle arrest, DNA damage response and autophagy in cancer cells. *Apoptosis* 2014; 19: 1389–98.
 - 27 Ng CP, Lee HC, Ho CW, Arooz T, Siu WY, Lau A, *et al*. Differential mode of regulation of the checkpoint kinases CHK1 and CHK2 by their regulatory domains. *J Biol Chem* 2004; 279: 8808–19.
 - 28 Smith J, Tho LM, Xu N, Gillespie DA. The ATM-Chk2 and ATR-Chk1 pathways in DNA damage signaling and cancer. *Adv Cancer Res* 2010; 108: 73–112.
 - 29 Clarke CA, Clarke PR. DNA-dependent phosphorylation of Chk1 and Claspin in a human cell-free system. *Biochem J* 2005; 388: 705–12.
 - 30 Kao J, Milano MT, Javaheri A, Garofalo MC, Chmura SJ, Weichselbaum RR, *et al*. gamma-H2AX as a therapeutic target for improving the efficacy of radiation therapy. *Curr Cancer Drug Targets* 2006; 6: 197–205.
 - 31 Sharma A, Singh K, Almasan A. Histone H2AX phosphorylation: a marker for DNA damage. *Methods Mol Biol* 2012; 920: 613–26.
 - 32 Xiao Y, Ramiscal J, Kowanetz K, Del Nagro C, Malek S, Evangelista M, *et al*. Identification of preferred chemotherapeutics for combining with a CHK1 inhibitor. *Mol Cancer Ther* 2013; 12: 2285–95.
 - 33 Klionsky DJ, Abdelmohsen K, Abe A, Abedin MJ, Beliovich H, Acevedo Arozena A, *et al*. Guidelines for the use and interpretation of assays for monitoring autophagy (3rd edition). *Autophagy* 2016; 12: 1–222.
 - 34 Park C, Suh Y, Cuervo AM. Regulated degradation of Chk1 by chaperone-mediated autophagy in response to DNA damage. *Nat Commun* 2015; 6: 6823.



This work is licensed under the Creative Commons Attribution-NonCommercial-No Derivative Works 3.0 Unported License. To view a copy of this license, visit <http://creativecommons.org/licenses/by-nc-nd/3.0/>

© The Author(s) 2017